J Therm Anal Calorim (2017) 130:2227–2238
DOI 10.1007/s10973-017-6610-z

Study on the evolution characteristic of intermediate during the pyrolysis of oil shale

Mengya Li[1,2] · Jin-Hui Zhan[1] · Dengguo Lai[1,2] · Yong Tian[1,2] · Xiaoxing Liu[1] · Guangwen Xu[1]

Received: 17 December 2016 / Accepted: 26 July 2017 / Published online: 17 August 2017

Abstract The pyrolysis of oil shale is a complex process including a myriad of chemical reactions. A widely approved understanding suggests a two-step decomposition process for oil shale pyrolysis, considering bitumen as the intermediate product. In this study, intermediates derived from various pyrolysis conditions are comprehensively studied by FTIR, GC, GC–MS and NMR methods to understand the pyrolysis mechanism of oil shale and composition feature of intermediate. The pyrolysis of oil shale is a dynamic process, and the results show that the intermediate is continuously generated before 400 °C, accompanying with the formation of final products from both intermediate and kerogen. The maximum yield of intermediates is presented at the fastest oil-producing temperature range (375 °C in this study). Carbon chains in intermediate become short with the increase in temperature. Most components in pyrolysis intermediate are long straight aliphatic chains; thus, intermediate is much heavier than shale oil. Further reactions make intermediate convert into shale oil product. Aliphatic hydrocarbons occupied the biggest proportion over 86% at 375 °C, mainly in the form of straight-chain alkanes. A few parts of aromatic fragments with small ring numbers will also transfer into intermediate. The heteroatom-containing compounds are mainly alcohols, ketones, amides and halohydrocarbons. High aromaticity in shale oil at high temperatures can be attributed to the condensation reaction of abundant aliphatic hydrocarbons in intermediate. During the conversion process from intermediate to final products, the generating capacity of oil is evidently higher than that of gas.

Keywords Oil shale · Intermediate · Pyrolysis · Structural composition

Introduction

As a solid fossil fuel with huge reserves, the utilization of oil shale can supply oil production and heat source by pyrolysis/retorting and direct combustion, respectively, which successfully keeps the sustainable energy security in many countries [1, 2]. Oil shale is more suitable for the production of shale oil by pyrolysis due to its higher H/C atomic ratio comparing with coal, which is favorable to produce high value-added oil. To obtain high quality of shale oil, it needs to reduce the aromaticity in oil and increase the yield of light oil. However, it is always very difficult to realize this goal due to thermal decompositions of organic matter in oil shale including a series of complex chemical reactions.

Considerable research efforts have been devoted to chemical kinetic models for quantifying the composition changes of shale oil. Burnham has summarized kinetics research achievements of oil and gas generation, indicating that the earliest model proposed by Hubbard and Robinson is the most commonly cited one [3]. Increased knowledge of oil shale kerogen structure with various advanced analytical methods such as advanced solid-state ^{13}C NMR, gas chromatography–mass spectrometry and infrared spectroscopy makes a further understanding of the reaction process for the

✉ Jin-Hui Zhan
jhzhan@ipe.ac.cn

✉ Guangwen Xu
gwxu@ipe.ac.cn

[1] State Key Laboratory of Multiphase Complex Systems, Institute of Process Engineering, Chinese Academy of Sciences, Beijing 100190, China

[2] University of Chinese Academy of Sciences, Beijing 100049, China

pyrolysis of oil shale [4–11]. A widely approved theory for the decomposition process of oil shale consists of two steps: (1) With the increase in temperature to around 350 °C [12, 13], kerogen decomposes and converts to solvent-extractable organic matter, which is defined as pyrolysis intermediate in this study. (2) Intermediate further decomposes and forms final products including gas, oil and solid residue [14]. Comparisons of chemical composition between intermediate and corresponding oil shale coupling with the analysis of other final products can help to reveal the oil shale pyrolysis mechanism in a different way. However, reports about systematic and detailed information about intermediate in terms of both pyrolysis mechanism and composition feature are rare. Braun et al. [14] reported the kinetic analysis of oil production in terms of two consecutive first-order reactions and considered the pyrolytic bitumen as intermediate production. Zaidentsal et al. [15] investigated the influence of temperature condition and isothermal exposure time on the yield of thermal intermediate and obtained the maximum yield of thermal bitumen at 390 °C. Li et al. [16] investigated the structural feature of organic intermediate obtained from Huadian oil shale at critical temperature of 350 °C and made a comparison with kerogen matrix. Williams [17] performed artificial maturation experiments to simulate thermal maturation of oil shale and found that bitumen played an intermediate role in the course of generating the final products. Despite the importance of intermediate in shale pyrolysis, its formation mechanism, difference with shale oil and chemical composition have not been investigated as much detailed as other oil shale products. On the acknowledgment of those rare studies, this paper presents a comprehensive study of intermediate and shale oil derived from various pyrolysis conditions, in order to get a particular understanding of pyrolysis intermediate by various characterization methods which have not been done in-depth so far, as well as oil-generating mechanism in terms of intermediate.

Experimental

Sample preparation

A kind of typical oil shale used in this study is obtained from Gonglangtou deposit located in Huadian, Jilin Province, China. For the primate preparation, the oil shale samples were crashed, ground and sieved to a small size of 0–2 mm and then dried in an oven at 105 °C for 24 h to eliminate the possible influence from water. The proximate and ultimate analysis of the Huadian oil shale is shown in Table 1. The ash content was 66.42 mass%, and the oil yield from Fischer Assay experiment was 9.98 mass% on dry basis. The atomic H/C was 1.87.

According to the thermogravimetry analysis of original oil shale at the heating rate of 10 °C min^{-1}, the mass loss peak began at around 300 °C with a relatively slow speed and reached the top at 450 °C, but the quick weightlessness region was at 350–400 °C, and the decomposition of organics was completed at 525 °C. Thus, pyrolysis temperatures were chosen from 300 to 525 °C to obtain comprehensive information about intermediate and shale oil. The pyrolytic experiments were conducted in a small furnace, and 80 g oil shale sample was used each time at the heating rate of 2° min^{-1} after fast heating up to 200 °C in 20 min. After that, the furnace was held at the corresponding temperature for 3 h and the remaining solid sample (named semicoke in this article) was taken out carefully and stored in drying vessel for the next procedure. Also, shale oil at each temperature was collected for the comparison with intermediate.

The extraction device used in this experiment was Soxhlet, and the solvent used here was chloroform due to the good solubility for bitumen [18]. Around 70 g semicoke was put in the tube each time, after that, the solvent was heated at 62 °C, and the extraction procedure was operated long enough until the siphon tube with solvent and intermediate presented transparent. Continuous extraction for 4 times at each temperature was employed here to get enough intermediate. At last, the final solution was evaporated in a rotator evaporation device to obtain pure pyrolysis intermediate for further analysis. Because the yield of intermediate was extremely low when the pyrolysis temperature was lower than 325 °C or higher than 425 °C, and its purification was almost impossible, we focused on the analysis for intermediates at 350, 375 and 400 °C, respectively.

Analysis and characterization

Elemental analysis of the samples was conducted using a Vario Macro cube Elementar. The results are shown in

Table 1 Proximate and ultimate analysis of Huadian oil shale properties of oil shale

Proximate analysis/mass%, dry basis			Ultimate analysis/mass%, dry basis					Fisher assay/mass%
A[a]	V[b]	FC[c]	C	H	N	S	O[d]	9.98
66.42	28.05	5.53	21.65	2.34	0.65	0.48	6.94	

[a] ash, [b] volatiles, [c] fixed carbon, [d] calculated by difference

Table 2 Ultimate analysis of intermediate

Pyrolysis temperature/°C	350	375	400
Ultimate analysis of intermediate/mass%			
C	83.74	82.92	84.36
H	11.53	10.74	10.21
N	0.72	1.09	0.79
S	1.18	0.84	0.88
O[d]	2.83	4.41	3.76
Atomic H/C ratio	1.65	1.55	1.45

[d] By difference

Tables 2 and 3, including the calculated atomic ratio of hydrogen and carbon atom (H/C).

Gas chromatograph (Agilent 7890B) was used here to characterize boiling point distribution of samples. GC–MS (Shimadzu QP2010 Ultra) with a capillary Rtx-5MS (30 m × 0.25 mm I.D. and 0.25 μm film thickness) was used for component analysis. The temperature program for the GC method started by holding at 50 °C for 5 min and then increased to 280 °C with a heating rate of 6 °C min^{-1} and then held for 10 min. The solvents used to dissolve the intermediate and shale oil were chloroform and acetone, respectively. In the MS program, the interface temperature was 280 °C, while the ion source temperature was 200 °C. The components were identified by matching with the NIST library and WILEY database. The relative concentration of every compound was calculated based on the integral of the corresponding peak areas and the total peak areas.

The FTIR analysis for the intermediate was performed using a Bruker Tensor 27 FTIR spectrometer. To prepare the sample pellets, the dry KBr was ground to fine powder first and pressed to disks for 10 mm diameter at 20 MPa for 30 s using a sample presser. Then the intermediate dissolved in chloroform was dropped at the center of the pellets. FTIR spectra for the sample were obtained with a resolution of 4 cm^{-1} and the spectral range of 4000–400 cm^{-1}. In order to eliminate the influence of solvent, the scan was conducted every 5 min, till the peaks caused by chloroform (1218 and 773 cm^{-1}) were disappeared.

High-resolution liquid-state NMR spectroscopy was performed using an Avance III spectrometer (Bruker Bio-Spin GmbH), operated at 700 MHz for ^{13}C NMR spectroscopy.

Results and discussion

Yield distribution of final pyrolysis products and intermediate

Yields of final pyrolysis products and pyrolysis intermediate extracted from semicoke were compared at different temperatures (all the yields were calculated based on original oil shale in this study). As shown in Fig. 1, yields of shale gas and pyrolysis water showed an upward trend, while yield of semicoke decreased with temperature increasing from 300 to 525 °C. Oil shale started to decompose and form shale oil at around 325 °C and yield of shale oil reached a maximum at 450 °C in this study. After 450 °C, yield of shale oil showed a decreasing trend, because the final pyrolysis temperature was relatively high, and the retention time for pyrolysis final temperature was long enough to ensure complete reaction, some volatiles cracked to form shale gas and pyrolysis water. This is supported by the appearance in Fig. 1 that yield of water and gas added the loss showed a shift to faster growth after 450 °C. Intermediate could only be obtained from 325 to 400 °C, and the yield first increased and then declined with the increase in temperature. The results indicated that during the generation of shale oil, intermediate played an important role: below 400 °C, it had to undergo an intermediate stage, because the temperature was too low to provide enough energy for the decomposition of kerogen and generating shale oil immediately; after 400 °C, shale oil was produced directly by the original organics of oil shale without experiencing intermediate stage at high

Table 3 Ultimate analysis of shale oil

Pyrolysis temperature/°C	350	375	400	425	450	475	500	525
Ultimate analysis of shale oil/mass%								
C	83.48	84.29	82.76	81.72	83.12	84.70	83.93	84.17
H	13.05	12.40	12.13	11.83	12.01	12.10	11.96	11.91
N	0.57	0.52	0.86	0.89	0.89	0.89	1.04	1.05
S	0.57	0.60	0.48	0.53	0.45	0.32	0.70	0.50
O[d]	2.33	2.19	3.77	5.57	3.53	2.00	2.37	2.37
Atomic H/C ratio	1.88	1.77	1.76	1.74	1.73	1.72	1.71	1.70

[d] By difference

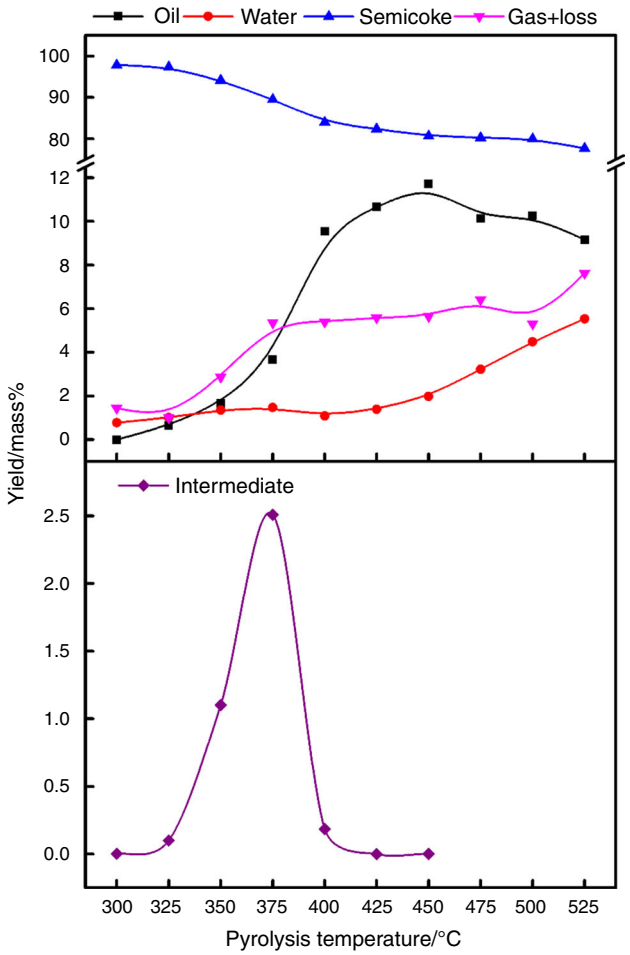

Fig. 1 Yields of final pyrolysis products and intermediate at various temperatures

temperatures, because the decomposition product of kerogen will volatilize rapidly or convert further to form final pyrolysis products.

Overall reaction process of oil shale pyrolysis

Generation and reaction characteristics of intermediate

The maximum yield of intermediate appeared at 375 °C, which was less than shale oil by 1.16% at the same temperature. Rate of oil producing was the highest at the temperature range from 350 to 400 °C, and shale oil produced between 350 and 400 °C accounted for 67.12% of the highest oil yield 11.71% at 450 °C. Interestingly, the maximum yield of pyrolysis intermediate was obtained at the same temperature scope of the maximum oil yield, agreeing with the results of other experimental studies [13, 19]. At higher temperature, the yield of intermediate started to abate sharply, which reduced to nearly zero at 400 °C, indicating that the intermediate can be produced beyond a certain temperature and can stably exist at a limited temperature boundary: the range of the highest rate of oil producing. Besides, direct pyrolysis products were generated at the same time as the formation of intermediate, but the intermediate could continuously convert to pyrolysis products, called parallel reactions in some studies [17, 19].

The results of ultimate analysis of intermediate and shale oil are listed in Tables 2 and 3, respectively. Because the yield of intermediate extracted from solid semicoke is extremely low when the temperature is lower than 350 °C or higher than 400 °C, we focus on the analysis of the intermediate extracted at the pyrolysis temperature of 350, 375 and 400 °C. When the pyrolysis temperature is lower than 400 °C, the heteroatoms N, S and O account for a higher proportion in intermediate than those in shale oil, showing that the heteroatom-containing fragments of oil shale kerogen can convert to shale oil partly at the early heating stage, and most of which exist in the form of intermediate. An estimation of the total heteroatom content in intermediate shows 1.36 and 1.92 times of that in shale oil at 350 and 375 °C, respectively, and only 35–45% of that is converted into shale oil. As Fig. 2 demonstrates, the atomic H/C ratio in intermediate and shale oil decreased with the increase in temperature, while the value of intermediate was much smaller than that of shale oil. Thus, the results indicate that in the course of intermediate converting to final pyrolysis products, the hydrogen-rich organics turn into shale oil while the contrary hydrogen-poor organics become semicoke. The value of H/C was evidently lower in semicoke than that in shale oil and in intermediate, suggesting that most of the hydrogen atoms are transferred into shale oil during secondary allocation. Besides, the atomic H/C of semicoke declined significantly with raising temperature and reached the bottom at 525 °C. Interestingly, after extraction the atomic H/C ratio of semicoke just had a slight change but still declined comparing with that before extraction at the corresponding temperature, which can be attributed to intermediate just accounting for a small proportion of semicoke before extraction.

Distillation fraction characterization for shale oil and intermediate

Shale oil and intermediate distillation fraction distribution was analyzed by GC, and the boiling point was categorized into four items with the gasoline <200 °C, diesel 200–350 °C, VGO 350–500 °C and heavy oil >500 °C. As shown in Fig. 3, diesel had the biggest proportion at all the operational temperatures, while a relatively small proportion was observed for gasoline, and heavy oil couldn't be detected in shale oil. With increase in the temperature, firstly, the relative content of diesel sharply decreased and

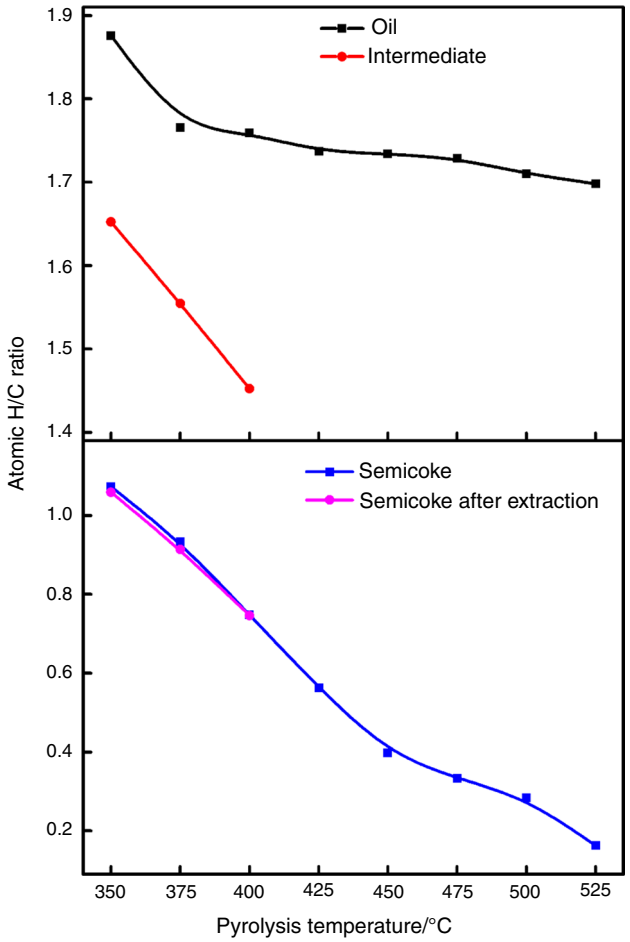

Fig. 2 Comparison of atomic H/C ratio at different temperatures in shale oil, intermediate, semicoke and semicoke after solvent extraction

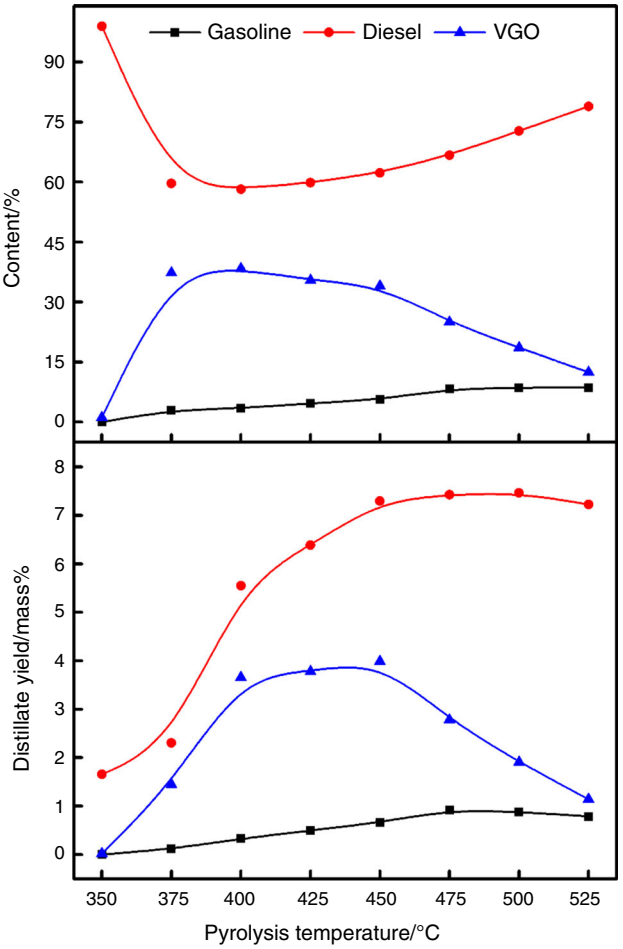

Fig. 3 Distillate content and yield of shale oil varying with temperature

reached the lowest point at 400 °C and then increased slowly between 400 and 525 °C. Interestingly, the content of VGO and diesel had the contrary tendency as the temperature rose, which indicated that VGO and diesel might be derived from the same fragments of kerogen, and formed under different reactions. The temperature window for the fast production of VGO located at 350–400 °C, which also could be transferred into diesel and gasoline by secondary cracking reactions when the pyrolysis temperature was over 400 °C. The cracking of the big molecules, such as the components of VGO, diesel and kerogen, may produce small fragments (gasoline or gas) under the long retention time and high temperatures.

The yields of distillate fraction in shale oil at different temperatures are also shown in Fig. 3. The yield of diesel was continuously increasing in the whole operational temperature range of this study, which kept at the level of about 7% with temperatures rising to 525 °C, while the yield of VGO increased at the low-temperature stage of 350–400 °C, then kept almost stable at the middle-temperature stage of 400–450 °C and decreased obviously at the high-temperature stage of 450–525 °C. For gasoline, the yield increased gradually until the temperature was elevated to 475 °C, after that the yield slightly decreased. However, the maximum yield of gasoline was still no more than 1%. From above results, we can conclude that the temperature below 400 °C is mainly the production stage of all the components of oil. The formation and decomposition ratio of VGO is almost equal at 400–450 °C, while the diesel yield is still increasing at the same temperature stage, suggesting that the decomposition of VGO can transfer into diesel. At higher-temperature stage of 475–500 °C, the amount for the decrease in VGO is much more than that for the increase in diesel and gasoline, which may be attributed to the systematic loss and the formation of gas and water, as shown in Fig. 1. The yield of diesel was not reduced as VGO and had a lifting trend, implying that part of big fragments of VGO may crack to form the smaller segments as diesel and gasoline before evaporating from the reactor.

Analysis of the distillate content and yields of distillation fraction for pyrolysis intermediate are shown in Fig. 4. The difference between intermediate and shale oil was that there were only VGO and heavy oil fractions in intermediate according to the categorized boiling points. Gasoline (boiling point <200 °C) and diesel (boiling point 200–350 °C) fractions had not been detected in pyrolysis intermediate based on the analysis of the simulated distillation GC. The difference demonstrates that components for pyrolysis intermediate are very heavy, and also implies the formation mechanism of intermediate that after critical temperature the relative weak bonds in kerogen crack to form long fragments but cannot escape from the 3D cross-linking structure of the kerogen and minerals. This cross-linking structure is so complicated that the fragments cannot further transfer into final products totally [9, 20]. It is well known that the decomposition of organic components starts at around 350 °C [16, 21, 22]. For this case, heavy intermediates were firstly formed significantly at 350 °C, and the content of VGO was higher than heavy oil, but the content of heavy oil exceeded VGO as the temperature elevated to 375 °C, which makes clear that the earliest cracking just needs less activation energy and the broken sites should be the most active ones in original kerogen. When the temperature increased to 400 °C, the content of heavy oil abated and the content of VGO exceeded the content of heavy oil. This change shows that higher temperature contributes to the decomposition of intermediate into smaller fragments.

As shown in Fig. 4, the yields of VGO and heavy oil both reached the highest at 375 °C, proving that the difference between the generation and consumption rates of intermediate reached a maximum value under this condition. The reason why there was a maximum yield at 375 °C is that during the fast oil-producing period, the rate of intermediate producing is much higher than that of intermediate consuming before 375 °C, but on the contrary after 375 °C. If the temperature is located at the fast oil-producing range, the total production of intermediate is always more than the total consumption; thus, intermediate can exist in the cross-linking structure of kerogen and minerals. If the temperature is higher than 400 °C, the production of intermediate is not enough for consuming, so the intermediate cannot exist instead, which will volatilize rapidly or convert further to generate final pyrolysis products.

The high-resolution ^{13}C NMR spectroscopy was performed to analyze aromatic and aliphatic carbon fractions in intermediate and shale oil collected at different temperatures, and the trends are shown in Fig. 5. The calculation method used in this study was by integrating the peak area where 0–90 ppm represents aliphatic carbons, 90–165 ppm represents aromatic carbons, and 165–220 ppm represents carbonyl carbons in ^{13}C NMR spectra. Aromatic carbon

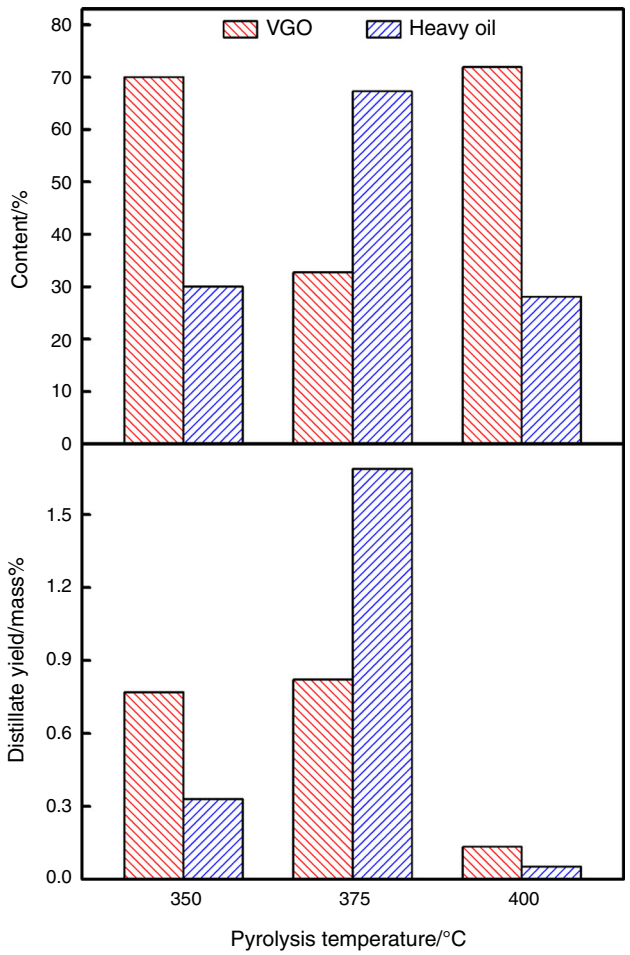

Fig. 4 Distillate content and yield of intermediate at different temperatures

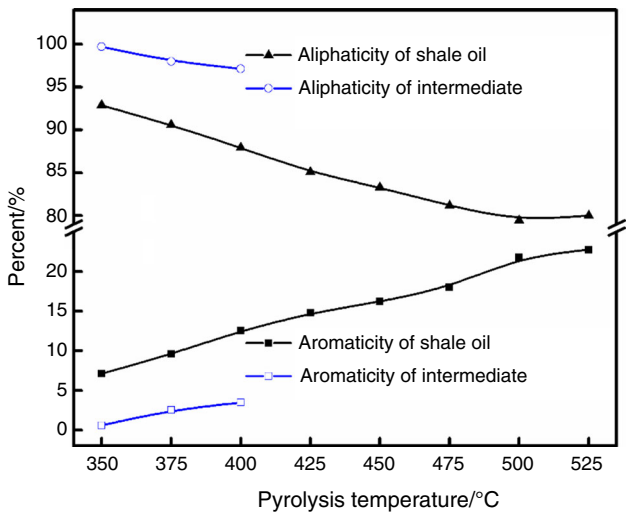

Fig. 5 Aromatic and aliphatic carbon fractions for the intermediate and shale oil collected at different temperatures

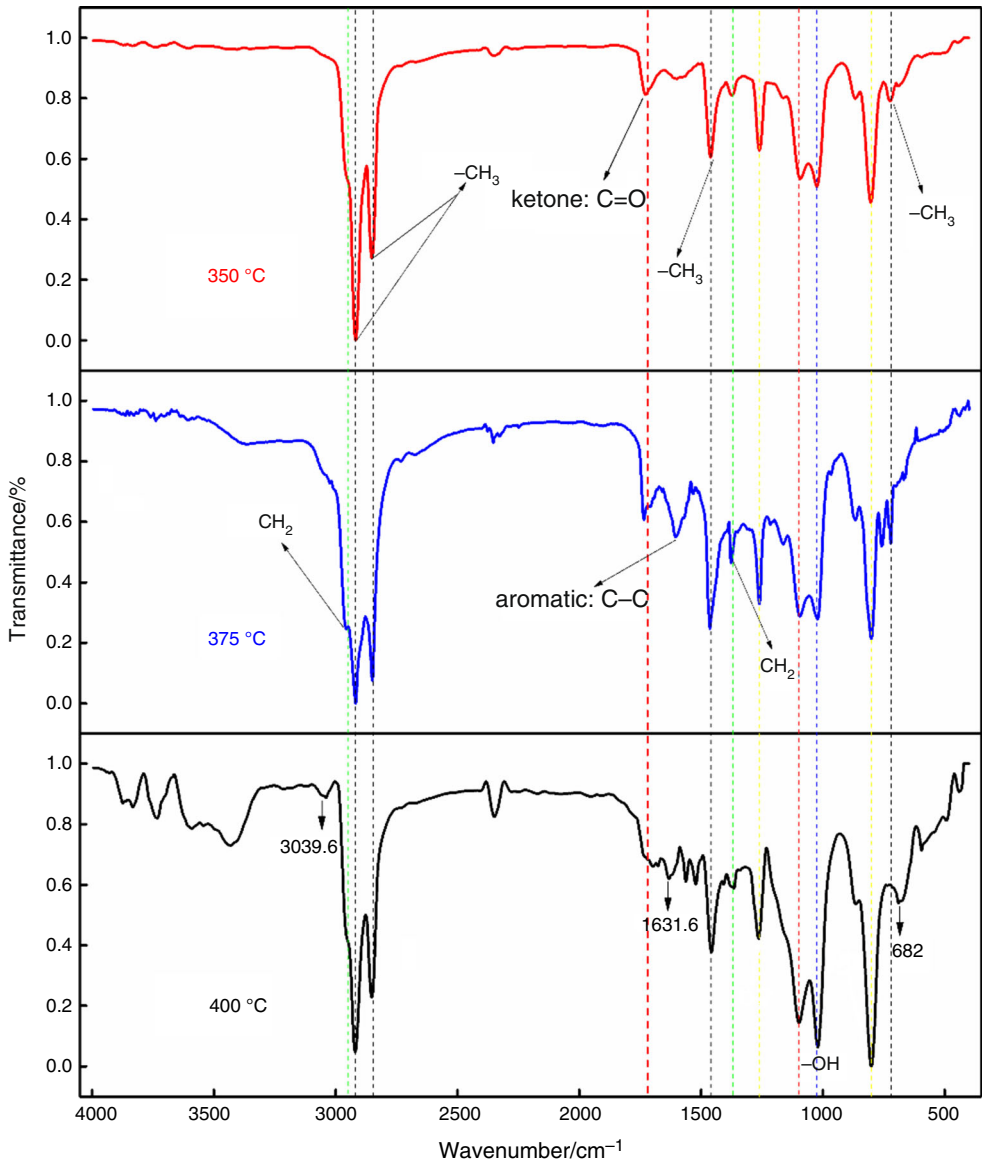

Fig. 6 FTIR spectra of the intermediate at 350, 375 and 400 °C, respectively

fraction in shale oil increased from 6.1 to 20% as the temperature increased, and the value for the intermediate increased from 0.3 to 2.86%, which indicates that aromaticity in shale oil is affected significantly by the pyrolysis temperature. Some studies documented that aromatic carbons in the original kerogen converted directly into oil with extremely low amount [23–25], and the amount of aliphatic carbons converting into residual carbon was very little, or the transfer of the two was equal. The aromatic fraction in intermediate was evidently lower than shale oil, which also shows undisputedly that the high aromaticity in shale oil at high temperatures can be attributed to the condensation reaction of abundant aliphatic hydrocarbons in intermediate.

Characterization of intermediate components

Information of functional groups in intermediate

The composition of functional groups in intermediate was investigated by using Fourier infrared method. The spectrum is presented in Fig. 6. There were mainly –CH_3, –CH_2, C=O, C=C, OH and –X(halogen) functional groups. The types of functional groups in intermediate extracted at different temperatures were nearly the same according to the detailed summary of FTIR adsorption peak positions of different functional groups from a variety of studies [26–29], but the difference of peak intensity in the same position implied the content of

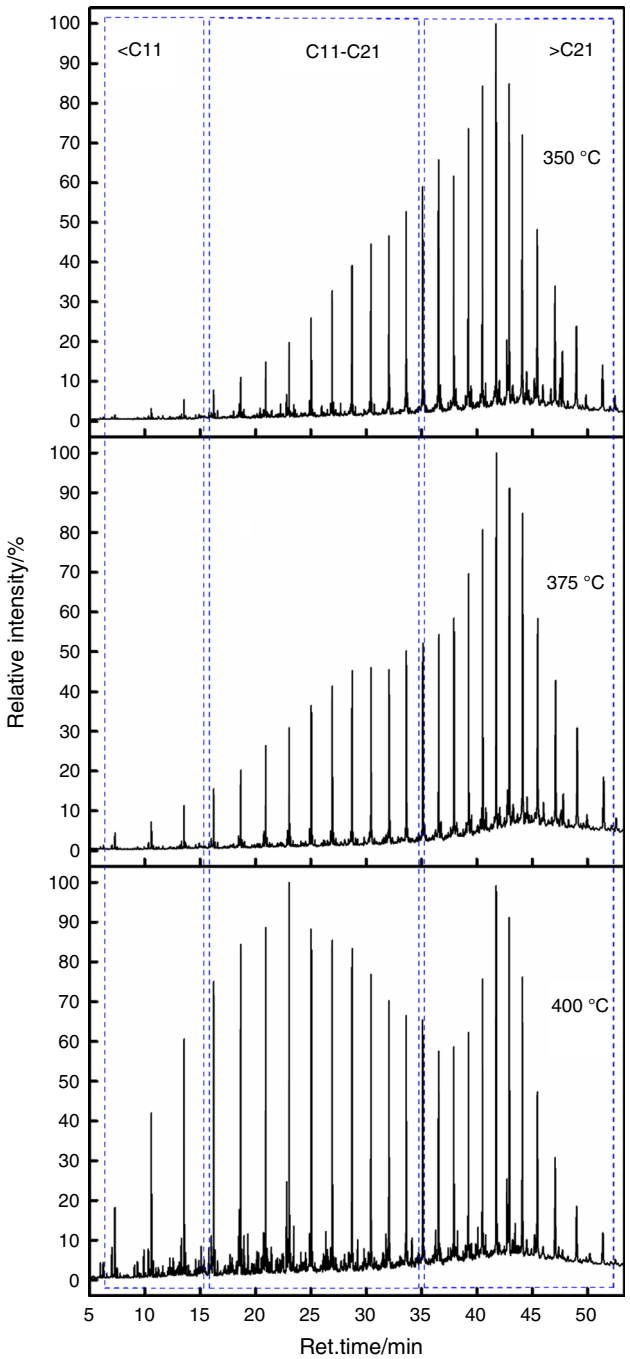

Fig. 7 GC–MS spectra of intermediate at temperature of 350, 375 and 400 °C

functional group was different. The strongest peaks at 2918.14, 2850.65, 1460.03, 721.34 (highlighted with black dash lines) and 2954, 1371 cm^{-1} (highlighted with green dash lines) shown in the FTIR spectrum are assigned to methylene and methyl, respectively. The peak at 1024.15 cm^{-1} (highlighted with blue dash line) belongs to C–OH stretching vibration of alcohols, and the peak highlighted with red dash line near 1726 cm^{-1} represent C=O stretching vibration from ketones together with the peaks of 1371 and 1099 cm^{-1}. A handful of ketones and alcohols were also detected by GC–MS, which was in good consistency with FTIR data. The aromatic C–H stretching vibration (3000–3100 cm^{-1}) was ambiguous, but peaks from aromatic C–C stretching vibration band at 1604.6 cm^{-1} could confirm aromatic hydrocarbon structure. Besides, it is obvious in Fig. 6 that the peak intensity of ketones (C=O) relative to aromatic hydrocarbons (C–C) decreased with increase in the temperature, indicating that the relative content of ketones abated comparing with the aromatic hydrocarbons. Absorption peak over 3300 cm^{-1} had a wide distribution and the intensity was relatively low, possibly resulted from associated OH or water (KBr from sample preparation was hydrophilic) stretching vibration band.

Composition of intermediate at 375 °C

As shown in Fig. 7, the components detected by GC–MS analysis in intermediate can be categorized as $<C_{11}$, C_{11}–C_{21} and $>C_{21}$ based on the number of carbon atoms in these compounds. Most of the peaks in GC–MS spectra were the same for the intermediates derived at different temperatures, but the relative intensity of the corresponding peaks changed as the temperature increased. The intensity of the peaks located in $<C_{11}$ and C_{11}–C_{21} intensified with increasing pyrolysis temperature, implying that the conversion of big molecular weight hydrocarbons to small molecular weight ones takes place at the temperatures of generating intermediates, which is in good consistent with distillation analysis for intermediate that higher temperature contributes to the decomposition of intermediate into smaller fragments. The maximum yield of pyrolysis intermediate was found at 375 °C, and the detailed component distribution was analyzed to understand the characteristic of intermediate. The strongest 100 peaks were picked out to match with the database of mass spectrum for identification of the molecular and structural formula of each peak.

Tables 4–6 list the relative content of aliphatic hydrocarbons, aromatic hydrocarbons and heteroatomic compounds calculated as the ratio of each peak area to the total peak areas in the mass spectrum of 375 °C. The most abundant components were aliphatic hydrocarbons which reached up to 85%, including straight alkanes, cycloalkanes, branched cycloalkanes and straight alkenes. Besides, there was a complicated unsaturated aliphatic hydrocarbon hop-22(29)-ene. No branched alkanes or alkenes were detected by GC–MS analysis for intermediate. Among all the aliphatic hydrocarbons, straight-chain alkanes occupied the highest content of 81.93%, which indicates that most structure in pyrolysis intermediate is long straight aliphatic

Table 4 Aliphatic compound distribution in intermediate at 375 °C

Compounds	Molecular formula	Relative content (Area %) 375 °C
Nonane	C_9H_{20}	0.24
Undecane	$C_{11}H_{24}$	1.07
Dodecane	$C_{12}H_{26}$	0.91
Tetradecane	$C_{14}H_{30}$	1.57
Pentadecane	$C_{15}H_{32}$	3.14
Heptadecane	$C_{17}H_{36}$	4.86
Heneicosane	$C_{21}H_{44}$	12.10
Tetracosane	$C_{24}H_{50}$	22.74
Dotriacontane	$C_{32}H_{66}$	3.26
Hexatriacontane	$C_{36}H_{74}$	29.73
Tetracontane	$C_{40}H_{82}$	2.31
1-Tridecene	$C_{13}H_{26}$	0.33
1-Tetradecene	$C_{14}H_{28}$	0.16
1-Pentadecene	$C_{15}H_{30}$	0.14
1-Heptadecene	$C_{17}H_{34}$	0.74
1-Nonadecene	$C_{19}H_{38}$	0.58
9-Hexacosene	$C_{26}H_{52}$	1.03
Cyclotetradecane	$C_{14}H_{28}$	0.32
Cyclohexadecane	$C_{16}H_{32}$	0.13
Dodecylcyclohexane	$C_{18}H_{36}$	0.15
n-Heptadecylcyclohexane	$C_{23}H_{46}$	0.36
15-Isobutyl-(13.alpha.H)-isocopalane	$C_{24}H_{44}$	0.20
Cyclopentane, heneicosyl-	$C_{26}H_{52}$	0.46
Hop-22(29)-ene	$C_{30}H_{50}$	0.36
Total		86.89

Table 5 Aromatic compound distribution in intermediate at 375 °C

Compounds	Molecular formula	Relative content (area %) 375 °C
Naphthalene, 1-methyl-	$C_{11}H_{10}$	0.19
Benzene, octadecyl-	$C_{24}H_{42}$	0.25
Benzene, [3-(2-cyclohexylethyl)-6-cyclopentylhexyl]-	$C_{25}H_{40}$	0.22
Benzene, nonadecyl-	$C_{25}H_{44}$	0.17
Benzene, eicosyl-	$C_{26}H_{46}$	0.31
Benzene, 1,3-didecyl-	$C_{26}H_{46}$	0.19
Total		1.34

chains. C_{24} compound tetracosane and C_{36} compound hexatriacontane were found in high content among all compounds classified by the carbon number. Among all alkanes, C_{21}–C_{36} compounds dominated in intermediate but according to analysis of shale oil at 375 °C, C_{20}–C_{24} compounds occupied the main part in oil products, indicating that further reactions occurred during the conversion process from intermediate to oil. Early study of kerogen

Table 6 Heteroatomic compound distribution in intermediate at 375 °C

Compound	Molecular formula	Relative content (Area %) 375 °C
n-Nonadecanol-1	$C_{19}H_{40}O$	0.19
Behenic alcohol	$C_{22}H_{46}O$	0.15
1-Heptacosanol	$C_{27}H_{56}O$	0.23
1-Octacosanol	$C_{28}H_{58}O$	0.20
1-Hentetracontanol	$C_{41}H_{84}O$	0.29
2-Pentadecanone	$C_{15}H_{30}O$	0.44
2-Heptadecanone	$C_{17}H_{34}O$	0.19
2-Nonadecanone	$C_{19}H_{38}O$	1.10
2,4,7,14-Tetramethyl-4-vinyl-tricyclo[5.4.3.0(1,8)]tetradecan-6-ol	$C_{20}H_{34}O$	0.14
Carbonic acid, octadecyl propyl ester	$C_{22}H_{44}O_3$	0.55
22-Tricosenoic acid	$C_{23}H_{44}O_2$	0.18
Heptadecanenitrile	$C_{17}H_{33}N$	0.99
Nonadecanenitrile	$C_{19}H_{37}N$	3.15
13-Docosenamide, (*Z*)-	$C_{22}H_{43}NO$	0.69
Hexadecane, 1-chloro-	$C_{16}H_{33}Cl$	2.18
Pentadecyl pentafluoropropionate	$C_{18}H_{31}F_5O_2$	0.23
Pentafluoropropionic acid, hexadecyl ester	$C_{19}H_{33}F_5O2$	0.32
Octadecyl pentafluoropropionate	$C_{21}H_{37}F_5O_2$	0.23
Nonadecyl pentafluoropropionate	$C_{22}H_{39}F_5O_2$	0.16
Docosane, 1,22-dibromo-	$C_{22}H_{44}Br_2$	0.13
Total		11.77

structure found that the overwhelming structure in oil shale kerogen was aliphatic carbon, and most of them were straight chains [30]. Our study shows that these long straight-chain compounds in intermediate are very likely to be the main structure of kerogen, which are easily released from the skeleton structure by pyrolysis. In previous studies, the aromatic hydrocarbons in shale oil were found to be mainly single- and double-ring compounds with aliphatic chains, which can be derived from paraffinic and naphthenic hydrocarbons by a series of pyrolysis reactions, such as cracking, dehydrogenation or cyclization. While the aromatic carbons in original kerogen tended to convert into shale char [3, 24, 25, 31, 32], the content of cycloalkanes and alkenes were very low and the majority of them possessed no branch.

The content of aromatics compounds detected by GC–MS was extremely low of only 1.34% in intermediate at 375 °C, further demonstrating that the aromatic structures in kerogen tended to convert into residue. The aromatic structures in pyrolysis intermediates were both single and double aromatic rings with branches. The double aromatic ring compound was 1-methyl-naphthalene, and the methyl

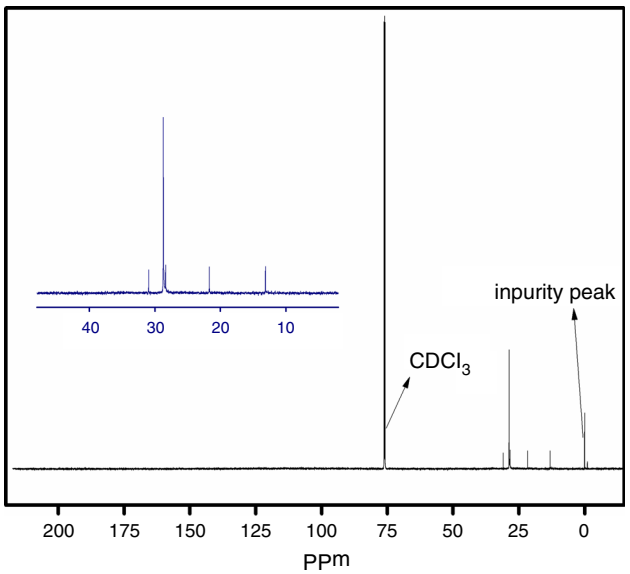

Fig. 8 ^{13}C NMR spectrum of intermediate extracted at 375 °C

substitute could be formed by beta-scission reaction of long side chain. Since the C–C bond located in beta site was easily broken down to form a radical with a methylene group, after bounding to a hydrogen atom, a new aromatic compound with a methyl substitute was formed and released from the kerogen [33].

Heteroatom compounds in pyrolysis intermediates mainly consisted of oxygen-, nitrogen- and halogen-containing compounds according to GC–MS analysis. They existed in the forms of alcohol, ketone, nitrile, halohydrocarbon and small quantity of ester-, acid-, amide- and fluorine-containing components. The oxygen-containing components were primarily consisted of alcohol, ketone and ester, which were in accordance with that in shale oil. Halogen-containing compounds were detected in GC–MS, further verifying the belonging groups of the absorption peaks at 1265 and 802 cm^{-1} in FTIR analysis. Nitrogen-containing compounds mostly existed in the form of nitrile with straight-chain molecular structure, and pentanenitrile and octanenitrile were also found in shale oil in other study [33].

The ^{13}C NMR spectrum of intermediate extracted at 375 °C is illustrated in Fig. 8, together with the partial enlarged curve between 0 and 50 ppm. The peaks at 77 ppm are assigned to deuterated solvent $CDCl_3$. Carbon types were categorized based on previous studies [5–7, 16, 34–38], and the content of each carbon type was calculated by integrating the corresponding peaks or regions, as shown in Table 7. The main components of intermediate are aliphatic compounds, with a few aromatic compounds. Thus, in the liquid-state ^{13}C NMR spectrum, the signal of aromatic carbons was faint, nearly coincided with the baseline. By integrating corresponding peak area for aromatic carbons, there were only 2.0% of aromatic carbons, suggesting a low aromaticity in intermediate. Similarly, carbons bonded to oxygen were also rare in

Table 7 Distribution of various carbons in intermediate at 375 °C

Carbon type	Location	Chemical shift/ppm	Temperature 375 °C Content/%
Carboxyl and carbonyl	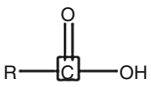	165–210	0
	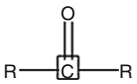		
Aromatic carbon	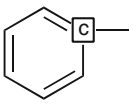	90–165	2.44
Methine and methylene		31.94	4.70
	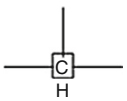	29.71	69.92
	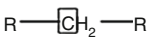	29.67	
		29.37	11.17
Methylene carbon bonded to methyl	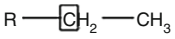	22.7	6.19
Aliphatic methyl	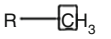	14.12	5.58
Aromaticity/%		90–165	2.44
Aliphaticity/%		0–90	97.56

intermediate (as mentioned before that ketones can be detected in FTIR and GC–MS, but the content was extremely low), and their peak areas were zero. Most carbons were belonging to methylene, implying that there are a lot of long straight chains. Among all the aliphatic carbons, aliphatic methyl carbons and methylene carbons bonded to methyl at 14.12 and 22.7 ppm, respectively, pertained to gas potential carbons, while methylene carbons bonded to methyl, methine and methylene carbons at 29.37, 29.67, 29.71 and 31.94 ppm pertained to oil potential carbons [25, 39, 40]. There are 11.77% gas potential carbons and 85.79% oil potential carbons based on the analysis of ^{13}C NMR spectrum, which can be converted into final pyrolysis products. Therefore, the capacity of generating oil is much higher than that for generating gas, and only a small number of intermediate will crack to form shale gas.

In general, intermediate is closely connected to both oil shale kerogen and final pyrolysis products. When the pyrolysis temperature is low, weak bonds in kerogen crack first to form heavy components, which exist stably in the form of intermediate in semicoke. Intermediate is mainly composed of long straight aliphatic hydrocarbons, and distillation fractions include VGO and heavy oil, whereas diesel and VGO fractions are predominant in shale oil, which is quite different with that of intermediates. However, when the pyrolysis temperature is high, intermediate can convert rapidly further to form final pyrolysis products. Especially, aliphatic hydrocarbons in intermediate undergo the condensation reaction to generate aromatic hydrocarbons in shale oil.

Conclusions

A comprehensive study of Huadian oil shale pyrolysis intermediates extracted at various temperatures is presented here. By ultimate analysis, FTIR analysis, GC, GC–MS detection and ^{13}C NMR spectroscopy, detailed results about the generation and reaction process of pyrolysis intermediates and their structural feature are discussed and summarized as follows:

(1) The intermediate can be produced beyond a certain temperature and can stably exist at a limited temperature range of 350–400 °C (the stage of the highest rate for oil producing). The maximum yield of intermediate appeared at 375 °C in this case. Pyrolysis oil and gaseous products will be also generated at the same time as the formation of pyrolysis intermediates, and the intermediate can continuously convert to pyrolysis products. The atomic H/C ratio of intermediates was much smaller than that of shale oil. In the course of converting intermediates to final pyrolysis products, the hydrogen-rich organics turn to shale oil while the hydrogen-poor organics become residue.

(2) There were mainly $–CH_3$, $–CH_2$, C=O, C=C, OH and –X (halogen) functional groups detected by FTIR spectra for the pyrolysis intermediates extracted at different temperatures. The relative content of ketones abated comparing with the aromatic hydrocarbons. Carbon chains in intermediate become short with the increase in temperature, according to the GC–MS analysis. Among all the hydrocarbons, straight-chain alkanes occupied the highest content 81.93%, and among all alkanes, C_{21}–C_{36} compounds dominated in intermediate but C_{20}–C_{24} occupied the main part in oil products at 375 °C. High aromaticity in shale oil at high temperatures can be attributed to the condensation reaction of abundant aliphatic hydrocarbons in intermediate. Aromatic hydrocarbons were single and double aromatic rings with branches. In the course of converting intermediate to final pyrolysis products, the capacity of generating oil is much higher, and only a small number of intermediate will crack to form shale gas.

Acknowledgements The authors gratefully acknowledge financial supported by the National Natural Science Foundation of China (21306210) and the National Basic Research Program of China (2014CB744302).

References

1. Xie FF, Wang Z, Lin WG, Song WL. Study on thermal conversion of Huadian oil shale under N_2 and CO_2 atmosphere. Oil Shale. 2010;27:309–20.
2. Barkia H, Belkbir L, Jayaweera SAA. Thermal analysis studies of oil shale residual carbon. J Therm Anal Calorim. 2004;76:615–22.
3. Burnham AK. Chemistry and kinetics of oil shale retorting. Oil shale A solut liq fuel dilemma. 2010;103:115–34.
4. Budinova T, Razvigorova M, Tsyntsarski B, Petrova B, Ekinci E, Yardim MF. Characterization of Bulgarian oil shale kerogen revealed by oxidative degradation. Chem Erde-Geochem. 2009;69:235–45.
5. Tong JH, Han XX, Wang S, Jiang XM. Evaluation of structural characteristics of Huadian oil shale kerogen using direct techniques (Solid-State ^{13}C NMR, XPS, FT-IR, and XRD). Energy Fuels. 2011;25:4006–13.
6. Ru X, Cheng ZQ, Song LH, Wang HY, Li JF. Experimental and computational studies on the average molecular structure of Chinese Huadian oil shale kerogen. J Mol Struct. 2012;1030:10–8.
7. Salmon E, Behar F, Hatcher PG. Molecular characterization of Type I kerogen from the Green River Formation using advanced NMR techniques in combination with electrospray ionization/ultrahigh resolution mass spectrometry. Org Geochem. 2011;42:301–15.
8. Zeng Y, Wu C. Raman and infrared spectroscopic study of kerogen treated at elevated temperatures and pressures. Fuel. 2007;86:1192–200.
9. Yan JW, Jiang XM, Han XX, Liu JG. A TG–FTIR investigation to the catalytic effect of mineral matrix in oil shale on the pyrolysis and combustion of kerogen. Fuel. 2013;104:307–17.
10. Wang W, Ma Y, Li SY, Yue CT, Wu JX, Teng JS. Prolysis characteristics of Longkou oil shale under optimized condition. J Therm Anal Calorim. 2016;125:983–90.

11. Wang ZJ, Liu XX, Wang YF, Liu LJ, Wang HY, Deng SH, Sun YH. Studies on the co-pyrolysis characteristics of oil shale and spent oil shale. J Therm Anal Calorim. 2016;123:1707–14.
12. Tiikma L, Zaidentsal A, Tensorer M. Formation of thermobitumen from oil shale by low-temperature pyrolysis in an autoclave. Oil Shale. 2007;24:535–47.
13. Wen CS, Kobylinski TP. Low temperature oil shale convention. Fuel. 1983;62:1269.
14. Braun RL, Rothman AJ. Oil-shale pyrolysis: kinetics and mechanism of oil production. Fuel. 1975;54:129–31.
15. Zaidentsal AL, Soonea JH, Muonib RT. Yields and properties of thermal bitumen obtained from combustible shale. Solid Fuel Chem. 2008;42:74–9.
16. Li QY, Han XX, Liu QQ, Jiang XM. Thermal decomposition of Huadian oil shale. Part 1. Critical organic intermediates. Fuel. 2014;121:109–16.
17. Williams PFV. Thermogravimetry and decomposition kinetics of British Kimmeridge clay oil shale. Fuel. 1985;64:540–5.
18. Tiikma L, Johannes I, Luik H, Lepp A, Sharayeva G. Extraction of oil from Jordanian Attarat oil shale. Oil Shale. 2015;32:218–39.
19. Wang Q, Sun BZ, Hu AJ, Bai JG, Li SH. Pyrolysis characteristics of Huadian oil shales. Oil Shale. 2007;24:147–57.
20. Wang Q, Sun B, Liu HP, Bai JR, Xiao GH. Analysis of mineral behavior during pyrolysis of oil shale. J Fuel Chem Technol. 2013;40:107–11.
21. Jiang H, Song L, Cheng Z, Chen J, Zhang L, Zhang M, Hu M, Li J, Li J. Influence of pyrolysis condition and transition metal salt on the product yield and characterization via Huadian oil shale pyrolysis. J Anal Appl Pyrolysis. 2015;112:230–6.
22. Bai FT, Guo W, Lü XS, Liu YM, Guo MY, Li Q, Sun YH. Kinetic study on the pyrolysis behavior of Huadian oil shale via non-isothermal thermogravimetric data. Fuel. 2015;146:111–8.
23. Rouxhet P, Robin P, Nicaise G. Characterization of kerogens and of their evolution by infrared spectroscopy: carbonyl and carboxyl groups. Geochim Cosmochim Acta. 1978;42:1341–9.
24. Miknis FP, Szeverenyi NM, Maciel GE. Characterization of the residual carbon in retorted oil shale by solid-state ^{13}C N.M.R. Fuel. 1982;61:341–5.
25. Qin K. Evolution model and evaluation method of organic carbon in oil shale. Oil Gas Geol. 1985;6:288–99.
26. Brewer CE, Schmidt-Rohr K, Satrio JA, Brown RC. Characterization of biochar from fast pyrolysis and gasification systems. Environ Prog Sustainable Energy. 2009;28:386–96.
27. Scholze B, Meier D. Characterization of the water-insoluble fraction from pyrolysis oil (pyrolytic lignin). Part I. PY–GC/MS, FTIR, and functional groups. J Anal Appl Pyrolysis. 2001;60:41–54.
28. Wei L, Mastalerz M, Schimmelmann A, Chen YY. Influence of Soxhlet-extractable bitumen and oil on porosity in thermally maturing organic-rich shales. Int J Coal Geol. 2014;132:38–50.
29. Simons WW, editor. The Sadtler handbook of infrared spectra. Philadephia: Sadtler research laboratories; 1978.
30. Wang Q, Huang ZY, Chi MS, Shi JX, Wang ZC, Sui Y. Chemical structure analysis of oil shale kerogen. CIESC J. 2015;66:1861–6.
31. Rovere CE, Crisp PT, Ellis J, Bolton PD. Chemical characterization of shale oil from Condor, Australia. Fuel. 1983;62:1274–82.
32. Fookes CJR, Duffy GJ, Udaja P, Chensee MD. Mechanisms of thermal alteration of shale oils. Fuel. 1990;69:1142–4.
33. Lai DG, Shi Y, Geng S, Chen ZH, Gao SQ, Zhan J-H, Xu GW. Secondary reactions in oil shale pyrolysis by solid heat carrier in a moving bed with internals. Fuel. 2016;173:138–45.
34. Wang Q, Jia CX, Ge JX, Guo WX. ^{1}H NMR and ^{13}C NMR studies of oil from pyrolysis of Indonesian oil sands. Energy Fuels. 2016;30:2478–91.
35. Fletcher TH, Gillis R, Adams J, Hall T, Mayne CL, Solum MS, Pugmire RJ. Characterization of macromolecular structure elements from a Green River oil shale, II. Characterization of pyrolysis products by ^{13}C NMR, GC/MS, and FTIR. Energy Fuels. 2014;28:2959–70.
36. Kelemen SR, Afeworki M, Gorbaty ML, Sansone M, Kwiatek PJ, Walters CC, Freund H, Siskin M, Bence AE, Curry DJ. Direct characterization of kerogen by x-ray and solid-state ^{13}C nuclear magnetic resonance methods. Energy Fuels. 2007;21:1548–61.
37. Žujović Z, Srejić R, Vučelić D, Vitorović D, Jovančićević B. Structural analysis of Aleksinac oil shale kerogen by high-resolution solid-state ^{13}C N.M.R spectroscopy. Fuel. 1995;74:1903–9.
38. Trewhella MJ, Poplett IJ, Grint A. Structure of Green River oil shale kerogen: determination using solid state ^{13}C N.M.R spectroscopy. Fuel. 1986;65:541–6.
39. Tissot BP, Welte DH. Petroleum formation and occurrence. Petroleum formation and occurrence. Berlin: Springer; 1984. pp. 643–644.
40. Mei YF, Zhao X, Sun WF, Tang J, Qiao AX. Spectral analysis of coal tar from Xiaohuangshan region. Chin J Magn Reson. 2011;28:339–48.